Journal of Power Sources 336 (2016) 40–53

Contents lists available at ScienceDirect

Journal of Power Sources

journal homepage: www.elsevier.com/locate/jpowsour

Review article

A critical review on gas diffusion micro and macroporous layers degradations for improved membrane fuel cell durability

Francois Lapicque [a, *], Mariem Belhadj [a, b], Caroline Bonnet [a], Joël Pauchet [b], Yohann Thomas [b]

[a] Laboratoire Réactions et Génie des Procédés, CNRS-Université de Lorraine, BP 20451, 54001 Nancy, France
[b] Université Grenoble-Alpes - CEA-LITEN /DEHT, 17, rue Martyrs, 38054 Grenoble, France

HIGHLIGHTS

- Physical phenomena related to MPL on GDL within the fuel cell, are analysed.
- The role of MPL in fuel cell performance and durability has been reviewed.
- Mechanical and physicochemical degradation phenomena are discussed.
- Promising routes for more efficient MPL and GDL are given.

ARTICLE INFO

Article history:
Received 18 June 2016
Received in revised form
7 October 2016
Accepted 10 October 2016
Available online 20 October 2016

Keywords:
Microporous layer
Gas diffusion layer
Optimal water management
Degradation
Durability

ABSTRACT

Formerly considered as a secondary component of fuel cell, gas diffusion layers (GDLs) have been shown to have a key role in gas transport to the catalyst layers and in water management: in particular, the microporous layer (MPL) deposited on the diffusion substrate has an active part in water distribution in the membrane electrode assembly and in its efficient removal from the cell. In addition to its perfect design for the targeted application and in combination with the macroporous substrate (MPS), the MPL structure and physicochemical properties have to contribute to the cell durability, which is still considered as insufficient for larger, massive commercialisation of this energy conversion system. The paper is aimed at reviewing the main knowledge gained on the role of the MPL on GDL operation and durability, with investigation of degradation phenomena of both MPL and MPS, together with the role played by the MPL in mitigating the occurrence of degradation phenomena that can occur in the whole fuel cell. In addition to the reviewing purpose, original data on ex-situ degradation of GDL are presented.

1. Introduction

Degradation of fuel cells' components has been investigated and reported for at least two decades. Probably, the most often treated aspects are the degradation of the ionomeric material forming the membrane and the catalyst layers i.e. platinum particles and their carbon support. The case of gas diffusion layers (GDLs) seems to have been less investigated, and often-cited literature reviews such as those of Borup et al. [1] or Zhang et al. [2], are more focused on degradation mechanisms of the membrane or the electrodes than on GDLs. Development of GDLs has become of an increasing importance: while appearing a minor concern in comparison with catalytic layers and membrane in the last century, it has become clearer that the nature and the design of GDLs could highly contribute to the performance of the cell and to the durability of its components, in particular because gas transport from the distribution plates to the catalytic sites can also be hindered in PEMFC operation by poor management of water. Although degradation of GDL has been partly treated in former reviews [1–3], few reviews devoted to the durability issue of GDLs have been published up to now: in addition to two general contributions [4,5], Park et al.'s review [6] is worth mentioning.

A GDL consists of a macroporous substrate (MPS) – also called gas diffusion backing, GDB – consisting of a carbon paper, cloth or felt, and a microporous layer (MPL). Fixation of an MPL onto the MPS has been first imagined by Watanabe [7]: from the improved performance of the cell, this additional layer has gradually become

* Corresponding author.
E-mail address: francois.lapicque@univ-lorraine.fr (F. Lapicque).

http://dx.doi.org/10.1016/j.jpowsour.2016.10.037
0378-7753/

a “standard” in fuel cell technology, allowing increased performance [8,9], lower influence of the MPS scattering [10,11] and improved durability [12,13], along with improvement in its fabrication [14,15]. MPLs are often produced by deposition or printing of finer carbon particles suspended in an ink containing a binder (typically PTFE) [8,12,16,17]. The MPL actually forms an intermediate layer between the macroporous substrate and the catalytic layer, in particular in terms of pore size distribution. From its structure and its composition, the MPL must have a suitable hydrophobicity for optimal transport of reacting gases to the catalytic layer while avoiding flooding or excessive drying of the crucial part of the cell. As mentioned by many authors e.g. Ref. [18] and demonstrated by simulation of multiphase flows in complex structures [19], the MPL appears to force transport of water from the cathode GDL toward the anode compartment which favours its removal in case of high humidification of the gases or high current densities. Because water is produced at the cathode, sometimes the use of different GDLs is considered at the anode and the cathode, in the so-called “asymmetrical GDLs” arrangement [20]. Besides, the MPL contributes to minimization of the electrical contact resistance between the catalytic layer and the MPS [2,21].

Most investigations of degradation phenomena on GDL have been carried out on the whole component, in some cases without clear indication on whether the degradation studied concerned more the MPS or the MPL. The purpose of this review paper is to concentrate on the role of MPL on GDL operation and durability, with investigation of degradation phenomena of both MPL and MPS. When possible, the role played by MPLs in (hindering) the occurrence of degradation phenomena in the whole fuel cell has been also reviewed.

Degradation phenomena of GDLs are often described as being either mechanical or chemical. In this paper, is has been preferred to change the classification into mechanical and physicochemical degradation. The first group related to GDLs comprises compression, the effects of freezing-thawing conditions on these layers, and erosion by gas circulating at high velocity. In the second group of degradation phenomena, chemical dissolution upon soaking in liquid solutions is treated before electrochemical dissolution or degradation of the layer constituents. So depending on the stress applied to the GDL, very different types of damage can be observed e.g. reduced porosity, breakage of carbon fibres, delamination of layers, dissolution of carbon materials, dissolution or degradation of water-repellent materials, and surface oxidation of the carbon components. Nevertheless, prior to the description of degradation phenomena occurring in the GDL, it is useful to briefly remind the general background on GDLs in PEMFC, and the methods to be used for characterization of their properties and investigation of their degradation – i.e. for evaluation of the state of health of the cell or one of its components. In addition to acting as a critical review on GDL role and degradation mechanisms, the paper presents a couple of original data on GDLs degradation under various conditions obtained in our laboratories. Promising routes for higher fuel cell durability are finally given.

2. A brief background on GDL structure and design

2.1. Macroporous substrate

The efficiency of an MPL in cell operation is also dependent on the nature of its substrate which justifies a brief presentation of MPS. Macroporous substrates consist principally of carbon fibres produced from polyacrylonitrile pyrolysis and assembled in various forms [5,22–24]. In carbon papers [25,26] fibres are bound in a plane structure by a binding material such as polyvinylic alcohol then impregnated in a resin to reinforce the structure. The assembly obtained is submitted to heat treatment at 2000 °C for carbonization of the matrix. In carbon felts [27], cohesion of fibres is not exclusively in a plane and heat treatment is carried out at slightly lower temperature. Pore sizes in the two above MPS materials are in the order of 10–30 μm according to [24] but more often in the range 20–100 μm as in Ref. [5]. Carbon cloths have actually a highly heterogeneous structure, with bundles of tight fibres and space between the woven bundles [5,28], resulting in very broad pore size distributions. For carbon cloths [29,30], the heat treatment is performed at 1600 °C only, which is the cause of a lower resistance to corrosion. The three MPS grades exhibit appreciable hydrophobicity allowed by the carbonized resin, however after high temperature treatment, MPS are usually impregnated in a PTFE suspension before a final treatment at 350 °C for stabilisation of the F-containing matter by sintering of the thin PTFE film formed [11,15,17] Besides PTFE distribution has recently been shown to be far from uniform in the MPS matrix [31,32]. In addition to PTFE, other fluorinated compounds e.g. fluorinated ethylene propylene [33], perfluoroether [34] or PTFE in combination with other polymers [35], can be used for this purpose. More recently French scientists in CEA [36] suggested to graft aryl compounds onto the GDL carbon base by reduction of the corresponding diazonium salt. Besides, metallic porous layers or foams can be employed as MPS materials [37,38].

The compared performance of MPS is often described in the literature [39]. Generally speaking, carbon papers have a larger water uptake than other substrates because of the tortuosity of their structure and their auto hydrophobicity [12,40]: they are efficient diffusion media for gases with low humidity and at moderate current density. Carbon cloths allow more efficient removal of water and are then preferred at high relative humidity and high current densities. This difference induced by the MPS nature is still visible in the presence of an MPL attached on the MPS [41].

2.2. Microporous layers

As a matter of fact the MPL is not merely a layer directly attached to the MPS with a flat interface between the two layers. Actually because the size of the particles forming the MPL is at least one order of magnitude below the size of the pores of the MPS, some of the MPL particles cover the carbon fibres of the MPS, with possible modification of their hydrophobicity/hydrophilicity: this can contribute positively to the removal of water produced toward the bipolar plate [42]. Depending on the amount of the ink deposited, the MPL particles can only deposit on the external carbon fibres of the MPS, without changing significantly the thickness of the combined diffusion medium, or – as in most cases – form an additional layer of micrometric carbon particles. In such case, the pore size and the porosity can vary significantly from the inner part of the MPS, then in the peripheral area formed by fibres covered by carbon particles forming an intermediate zone, then in the “bulk” MPL (Fig. 1a). The thickness of this intermediate zone is governed by the viscosity of the ink and the solvent used. In addition, depending on the pressure applied after deposition during the MEA preparation and its installation and compression in the cell, the MPL can penetrate to some extent into the macroporous substrate [6] forming the penetration zone which improves the cohesion and the compactness of the MPL on the MPS (Fig. 1b).

2.2.1. Components of MPL and preparation mode

First MPL grades as developed by Watanabe [7], and later by Refs. [10] and [43], were manufactured from suspensions of acetylene black in the presence of an F-containing polymer e.g. PTFE or even Nafion. Alternatively other carbon materials can be employed

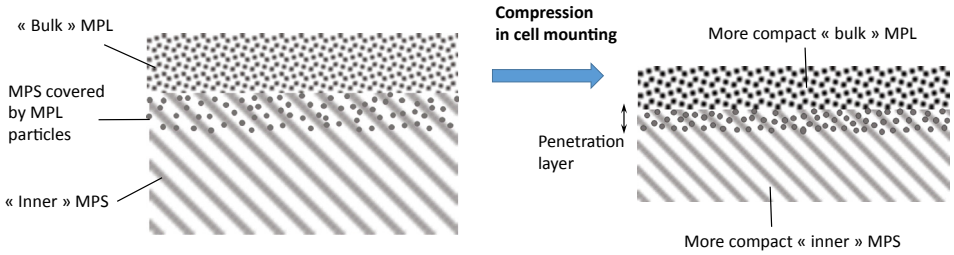

Fig. 1. Effect of compression on the structure of the various layers forming the GDL: (a) before compression, (b) after assembly and cell mounting.

e.g. carbon black, coke derivatives (metcoke), amorphous graphite or flake graphite. Most of these particles are prone to corrosion: replacement by graphitized particles of a stronger resistance, can therefore be preferred [44]. Also to be mentioned, the use of carbon nanotubes (CNT) in order to reduce the intensity of corrosion phenomena, as suggested for instance by in Refs. [34,45] and in Ref. [46]. Although often considered of high cost CNT have been proved within the EU-funded Impala project to be a viable solution to improve both fuel cell performance and durability. In addition to carbon-based materials, variable amounts of water-repelling agents and polymers can be incorporated: although PTFE remains the most commonly used agent, other F-containing compounds mentioned above for MPS preparation were also tested. Depending on the strategy developed and the targeted utilization of the GDL, the weight fraction of F-containing polymers can vary from 10 to 40% in MPLs: this aspect has been extensively discussed in published literature [11,15,33,47,48] and is not further commented here.

At the fringe of MPL technology, functionalization of the MPS surface by hydrophobic polymers e.g. perfluoropolyether [49] or PVDF [50] or even a titanium layer by direct current (magnetron) sputtering on the anode-side MPS [51] can be mentioned. In addition to the nature of the particles involved, the process for MPL preparation on the MPS surface (simple deposition, pulverization, printing or separate preparation before assembly on the MPS surface [36], has also an impact on the overall GDL properties: for instance as reported by Ref. [12], printed MPLs allow the presence of larger pores in the carbon particle matrix which is to ensure more efficient separation of vapour from liquid water. In addition, deposition of the MPL under reduced pressure was shown to favor the PTFE penetration and dispersion in the micropores of the carbon paper [52].

2.2.2. Role of MPL in transport and transfer phenomena

The structure of MPLs contains both macropores – above one micrometer or even far above – and micropores (in fact this is mainly mesopores below 0.1 μm). Nishiyama and Murahashi [53] showed that the so-called micropores are hydrophobic, suitable for gas transport whereas large pores can be hydrophobic or hydrophilic, depending on the MPL composition and the location in the layer (as schematically depicted in Fig. 2). Because of its far larger viscosity than for gases and its poor affinity to micropores, liquid water can only be transported in macropores. The rate of this transport is governed by the local surface properties and inertia forces. Transport of gas can occur in all pores with the only conditions that the duct is not locally plugged by liquid water.

The nature of transport phenomena is often discussed in the literature in an attempt to determine whether it is simple diffusion in a porous medium and described by Stefan-Maxwell equation as considered in Ref. [54] or whether convection has to be accounted for by using transport models derived from Darcy's law or by binary friction models, which are more suitable to describe Knudsen diffusivity in the MPL [55]. Transport phenomena in GDLs often involve the presence of gas and liquid, for which various approaches can be considered e.g. Leverett function, pore network model, Lattice Boltzmann model etc. More complete description of these approaches can be found in the literature [19,54,56–59]. Besides, because of its moderate volume flow rate in comparison to gases, water does not flow continuously in the cell layers but in the form of intermittent ejection, often called “eruptive transport” [60]: this particular flow mode results from the so-called “Haines jump”, corresponding to a pore scale interfacial jump [61,62]. In this complex flow mode, surface phenomena – at the microscale -, gravity and inertia forces at larger scales, have not been accounted for in the above models [60–62]. For this latter aspect, the usual assumption of capillary flow is justified by the small dimensions and the little/moderate significance of liquid water in the GDL.

The penetration depth has a significant effect on water removal by the MPL, as shown by Cho et al. [63]: as a matter of fact, high penetration depths can efficiently smoothen the profile of capillary pressure gradient – actually the driving force for water transport - which induces enhanced back diffusion flow from the GDL to the catalytic layer and the membrane, resulting in higher performance.

Besides, the MPL structure consisting of much finer particles than that of the MPS, exhibits a thermal conductivity approx. 5–10× lower than that of the macroporous support [64]. Therefore, the heat produced by electrode irreversibility and ohmic drop is removed at a finite rate through the MPL which can be the source of visible temperature differences between the electrode-membrane assembly and the MPS, as reported in Ref. [64]. With concern heat transfer, MPL can thus be considered as an additional resistance to heat transfer in the fuel cell [65].

To conclude this section, the two parts of the GDL have been actively, successfully developed for fifteen years for the sake of higher performance through better controlled water management in the fuel cell: this research based on combined materials sciences, polymers and physical chemistry could also be supported by the recent advances in multiphase transport phenomena in the two sub-layers. Nevertheless, the obtained advances were too rarely validated by investigation of their durability in a fuel cells in comparison to that of catalytic layers or membranes.

3. General comments on degradation issues in GDLs

3.1. Degradation protocols

Because of the expected long lifetime of fuel cells, it is often considered necessary to develop protocols of accelerated stress tests (AST) as expressed in the above cited reviews and by Schmittinger and Valladi [66]. It has to be mentioned that few papers report on the degradation of GDLs in a cell operated in “real” conditions of power production. Generally speaking the methodology in AST design has been derived from those for electrodes or membranes, taking into account their different nature and

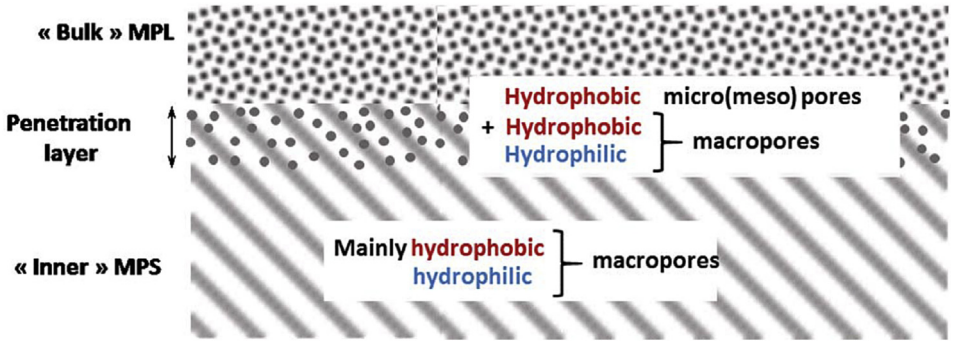

Fig. 2. Pores in the various regions of the GDL.

properties: in all cases, these AST are related to the various mechanical, thermal, chemical, electrochemical stresses in a fuel cell under operation. Two types of AST can be considered:

- In-situ AST, i.e. when the MEA is aged in the fuel cell in operation, however under most degrading conditions – presence of pollutants in the gases, current or potential cycling, cycling of relative humidity of the inlet gases, start and stop cycles. As for catalytic layers, potential cycling in particular at high levels
- Ex-situ AST: here the GDL is placed in an aggressive environment, either under mechanical or chemical stress [66]: for the latter case, the GDL can be immersed in an acidic solution for long periods [67]. Other ASTs consist in submitting the soaked GDL to highly anodic potentials in view to emulate start-and-stop conditions of the cell. Cycling the selected conditions enhances the stress applied to the component, as for other cell components. Likewise, for comparison of various GDL technologies, it is hoped that the difference in degradation extent and rates observed for the AST is representative of that under real fuel cell operation.

More accurate description of the various AST is given in Section 4 prior to the description of the facts reported and their interpretation.

3.2. Observation techniques for evaluation of the degradation extent

3.2.1. Direct (in-situ) evaluation

The most conventional techniques for evaluation of the GDL capacity are electrochemical tests of the mounted cells under regular operating conditions: (i) chronopotentiometric measurements at a given current density, with the transient response to sudden changes, and for which the presence of potential peaks or fluctuations reveals insufficient water management, (ii) the voltage vs current density curve recorded at steady state – which is a direct assessment of the cell performance, and whose suddenly decaying profile at high current density expresses strong control by mass transfer conditions, and (iii) impedance spectroscopy at a given current density (see for instance [68]): comparison of the diameter loops at high and low frequencies (in Nyquist plot) indicates on the change in charge and mass transfer rates respectively. However, the poor water management caused by an aged GDL may also impact on the electrode kinetics by insufficient hydration of the thin ionomer layer at the vicinity of the catalyst cluster together with higher ohmic resistance of the membrane.

3.2.2. Indirect (ex-situ) evaluation

In addition to the methods mentioned above, it is often necessary to carry out specific investigations on GDL analysed independently of the cell:

a) Electrochemical techniques, using the GDL as the working electrode in a three-electrode cell filled with an electrolytic solution (often dilute sulfuric acid). For instance, cyclic voltammetry in a potential range −0.2/0.8 V/SCE allows to estimate the significance of reversible oxidative processes on the GDL/MPL surface featuring quinone and hydroquinone groups near 0.4 V/SCE [69].
b) Physical methods
   - Measurements of the in-plane or through—plane electrical conductivity in a dedicated cell: decrease in the conductivity may express surface oxidation of the carbon surface or inner particles or partial delamination of the MPL from the substrate, but higher conductivities can be the fact of compressed MPS or MPL structures or the lack of fluorine-based water repelling agents deposited in their fabrication. Therefore the value of this physical property, although of a direct interest for the cell performance, does not always indicate on the modifications occurred at the GDL.
   - Measurement of the contact angle is a popular technique, consisting in observing a water droplet with a diameter in the order of 1 mm, deposited on the GDL surface and measuring its contact angle. A derived technique relies upon advancing then receding immersion of the GDL in water, measuring the weight to be applied for mechanical balance and analysis of the hysteresis curve [35,70], the contact angle can be derived from the weight applied. In all cases, the higher the angle value, the less affinity with water the surface exhibits. However, this information taken from the two techniques has to be taken with care because the investigated surfaces are far from flat and even [71] and the hydrophobic treatment of the surface may be not uniform. As a matter of fact, the roughness and the heterogeneity of the GDL surface – which can be aggravated by ageing - modify the wetting properties, so the measured, apparent contact angle may differ from the true contact angle [70]. This phenomenon is presumably more acute when the water droplet diameter is not significantly larger than the pore diameter or the roughness of the surface. Another limitation is that the contact angle measured reflects the property of the GDL surface and not of the GDL bulk volume.
   - Measurements of gas permeability through the GDL at a given pressure drop by using Darcy's law. Various experimental techniques have been developed [72,73] and this property is linked to the apparent diffusion coefficient of the gas in the medium as often discussed. Moreover interpretation of the measurements is governed by the model selected, as

explained in Ref. [55] in which both Darcy's law and binary friction model have been considered. Higher permeability may appear positive but is generally due to loss of carbon-based fillers or graphitized compounds on the GDL structure which is actually a real degradation. For the case of liquid water, only large pores are involved in their transport through the GDL: change in this permeability is mainly due to change in surface properties, in the present case, higher wettability of the GDL surface [74].

- Gas adsorption isotherm measurements using Brunauer–Emmett–Teller (BET) equation can indicate on the pore size distributions of the material investigated, MPS or MPL.

c) Thermogravimetric analysis

Thermogravimetric analysis consists in applying a temperature scan to a small material sample in an inert gaseous environment and in recording its weight along time. Scan rate is usually in the range 5–20 °C/min. The weight losses observed correspond to volatilization or decomposition of materials. In the present case, a shoulder exhibited in the range 500–650 °C is usually attributed to the decomposition of fluorinated polymers present in the GDL [22,69,75]. Comparison of profiles obtained with pristine and aged GDL can indicate on the loss of this polymer type by the stress applied to the GDL, as exemplified by Fig. 3. However, the accuracy of the determination is of the order of 1 wt%: since the amount of F-containing polymers is typically in the order of 10% in fresh GDL, only significant degradation can be indubitably evidenced with this technique.

d) Microscopic techniques

Scanning electron microscopy (SEM) can be used to observe the surface of the materials in conditions close to those experienced in the cell [76]. In addition to SEM, transmission electron microscopy (TEM) can also be employed for access – although not directly – to the sample surface to smaller entities. Quite often microscopic techniques are coupled to spectroscopic techniques as discussed in the following section. Various extensions of SEM are now available for diverse utilizations e.g. field emission (FE) SEM, SEM-focused ions beam (FIB) to image cross-sections of the GDL etc. [24,36]. More recently atomic force microscopy (AFM) has been used for microscale observations of the surface topography and morphology of fuel cell components. In the presence of media of very different conductivity – as in the present case with F-containing polymers and carbon black for instance, the nature of the local surface can be identified from the locally resolved conductivity [77].

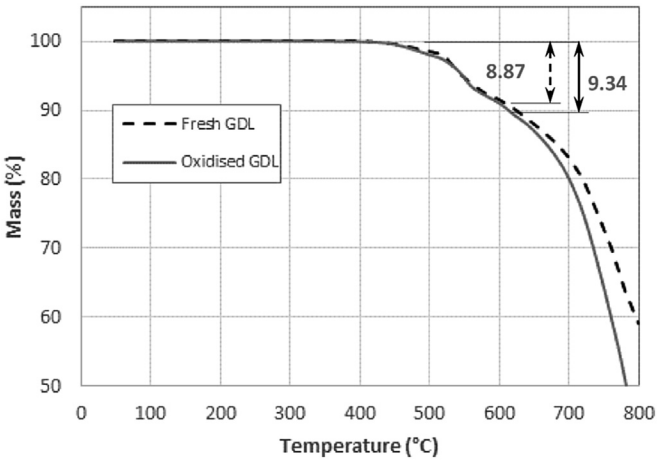

Fig. 3. Example of TGA measurements on GDL (adapted from Ref. [64]).

e) Spectroscopic techniques

These techniques can be used for both quantitative determination of water in the various layers of the cell, and chemical analysis of solid surfaces or leaching solutions in a semi quantitative manner.

3.2.3. Water determination

Confocal (micro) Raman spectroscopy is often employed to measure profiles of water concentration in the membrane of the cell considering the intensity of the O–H stretching band [78]. Several techniques involving far higher energy irradiation e.g. neutron imaging or synchrotron X-ray can be used for visualization purpose in operando fuel cell testing, as reviewed in Ref. [79]. Improvement of the techniques recently allowed higher temporal and spatial resolutions – at a few μm in the GDL [80]. X-ray tomography – also called "computed tomography" – derives from tomography, in a way that inside-views of the sample can be obtained without cutting the sample investigated, which allows for instance characterization of water saturation in GDL [81,82].

3.2.4. Chemical analysis

FT Infrared spectroscopy can be used for identification of the organic compounds present in the leaching solution and of the surface groups of the GDL: comparison of the spectra in the 500–4000 cm^{-1} range can evidence the presence of oxygenated groups – ether, alcohol or ketone functions on the surface created upon oxidative stress. Moreover non dispersive infrared (NDIR) spectroscopy of the exhaust gas can be used efficiently to measure the amount of CO_2 produced by (oxidative) degradation [44], with an accuracy far better than that exhibited by conventional gas chromatography.

More recently confocal Raman spectroscopy has been used in scanning cross sections of GDL in the Raman shift 500–2000 cm^{-1} [83]: the bands observed can reveal the various forms of carbon material (defect carbon, graphite etc.) at a selected position in the GDL: location, symmetry, broadness and intensity of the peak indicate in the nature of the carbon and its degree of crystallinity. Presence of other atoms can also be revealed but the intensity of the signals may be too low for clear evidence.

X-ray techniques are often coupled to SEM: energy-dispersive X-ray (EDX) allowing elemental analysis of the sample surface as done for instance in Ref. [36] to obtain the fluorine cartography. X-ray photoelectron spectroscopy (XPS) provides, in addition to the elemental composition, chemical state or electronic state of the elements from binding energy. For instance, significance of C–F, ether, alcohol or ketone functions can be determined by XPS. Also to be mentioned is electron-probe micro analysis (EPMA) where the solid surface is bombarded by an accelerated, focused electron beam, as reported in Ref. [35] for identification of the elements present on the GDL surface. Interestingly the authors coupled EPMA to time-of-flight secondary ion mass spectrometry (TOF-SIMS) as a complementary technique for identification of the substances adsorbed on this local surface showing for instance the presence of complex C, F, S and O unstable species created by the irradiation beam.

4. Mechanical degradation of GDLs

As expressed above, three main phenomena are presented in this section: compression, freezing-thawing and erosion.

4.1. Compression

GDLs are the components of the fuel cells exhibiting the highest porosity, which can attain in some cases 80%. Therefore they are the most prone to global or localized deformation, i.e. shrinking under the clamping pressure generated by mounting the fuel cell. Beyond the issue of degradation, the compression of GDL has three main effects:

- First, compression affects the gas permeability, as illustrated qualitatively in Fig. 2. For instance, 65% compression of the GDL can induce reduction of the permeability to the tenth of its initial value [84], with equivalent reduction in transport rates. Although less directly commented, permeability of water can also be affected, which could be detrimental to water management in the various fuel cell regions. Dotelli et al. [85] testing compressed MEA to 30% and 50% of their original thickness, observed lower performance and larger diffusion resistance at 50% compression. Overall, higher diffusion overpotentials and lower limiting current density can be expected.
- As often expressed [6], compression improves thermal and electrical contacts between the fibres forming the MPS and may favor the contact between the carbon particles of the MPL and the larger fibres: in addition to enhanced thermal and electrical conductivity, larger penetration depth of the MPL in the MPS can be expected.
- Compression to an acceptable level is also to favor the electrical contact between the various layers forming the cell: together with the above phenomena inside the GDL, this is to increase the overall conductivity of the structure by reducing the contact resistance between GDLs and bipolar plates [29].

These three effects have antagonistic impacts on fuel cell performance and a compromise between too low permeability of gases and liquid water and decreased ohmic drop is usually searched when preparing the MEA then mounting it in the cell. Whereas pre-compression of the MEA is to allow the controlled reduction in its thickness and the ex-situ evaluation of the GDL properties, this fundamental information may be no more valid after mounting the MEA in the cell at the torque recommended by the cell supplier. In most cases, the above phenomena are not to induce degradation issue, also because sufficient compression is required in a fuel cell. Nevertheless, localized damage can be observed, as commented in the following sub-section.

Compression of minor intensity can be reversible: each component returning to its pristine thickness as soon as the pressure is released. However in most cases, the deformation induced by the pressure applied on the cell components – in particular on the GDL – is irreversible, as observed by hysteresis in pressure cycling tests [86]. Repeated (cyclic) compression magnifies the amplitude of the irreversibility, then the induced degradation.

4.1.1. Localized compression

Compression of the various layers forming the active part of the fuel cell is more effective, and is sometimes the cause of degradation in two main parts of the cell: (i) in the peripheral zone of the MEA, i.e. in the vicinity of the bolts, in spite of the use of a gauged wrench; (ii) under the ribs of the flow patterns in the distribution plates: compression is more acute under the ribs, quite less under the channel under which the cross section of the channels offered to gas flow is presumably not perfectly rectangular because of appreciable GDL intrusion [87] (Fig. 4). In addition to the fact that compressed parts are more submitted to intense pressure than the rest of the cell area [5,88], it can be imagined that mechanical stresses are of a quite higher intensity at the edge of the ribs for instance, which is to result in formation of cracks in the GDL structure and other degradation. The intensity of the compression at the rib edge depends on the process used to produce the GDL: whereas machining and electrochemical machining can produce very sharp edges, progressive forming allows a larger radius of curvature.

4.1.2. Degradation by compression

At local scale in the GDL bulk, various degradation phenomena can occur under compression.

- First, as reported in many papers, carbon fibres forming the main part of the MPS can undergo appreciable breakage or even displacement in the fibres arrangement, which is to change the morphology of the overall structure, with possible consequences on current transport and permeability to fluids [87,89]. The physical and physicochemical properties of the GDL could be related to the mechanical degradation induced by compression [90,91], with in particular the effect of the fibre orientation on the overall ageing of the cell component.
- In addition, breakage of PTFE coating of the carbon fibres can also occur [79]. Over time, under the combined effects of blowing gas and liquid water, significant local losses of hydrophobicity can appear on their surfaces: this has been reported as a source of preferential transport pathway for water whose management can therefore be largely affected at local scale, either for water removal from its production source or for sufficient hydration of other areas.
- Besides, breakage of carbon fibres often being longer than 100 μm, can affect the surface roughness of the GDL, even on the MPL surface [90]. The stress induced the compression and in particular its non-uniform distribution has also an impact on the MPL structure, with formation of cracks on the surface.
- Moreover, displacement of carbon fibres induced by the local stress can be the cause of local damage at the ionomeric membrane: depending on the pressure applied and the GDL nature, Baik et al. [92] evidenced a significant increase in the fuel cross over – in relation to reduced open circuit voltage – which indicates appreciable degradation of the membrane. Local degradation of the catalyst layers is also to occur in such case.

In a general manner, heterogeneous structure of the MPS, i.e. non even arrangement of carbon fibres in this layer favours their mechanical degradation, either by breakage of the hydrophobic coating, or by breakage of fibres [93]: for this reason, the authors recommend the use of homogeneous carbon materials in both the MPS and the MPL for the sake of higher durability of the GDL.

4.2. Freeze-thaw

Freeze-thaw effects at MEA have been investigated for years because a major application of fuel cell technology is transport: fuel cells in cars or trucks parked for a long period of time in winter can suffer from ice formation in the various parts of the cell and at the component interfaces, generating localized expansion and causing local mechanical issues. This simple fact can render start-up of the fuel cell more complicated and, during the run-up of the cell, the ice formed melts to water, resulting in its back volume contraction. This phenomenon occurring repeatedly is known to alter the mechanical cohesion of the fuel cell components, with ongoing local delamination of the various cell layers: in the concerned areas, electrical contacts become looser and mass transport of the gas can be affected, the two effects resulting in poorer local performance [94–96]. The structure of the MPS has an impact on the durability

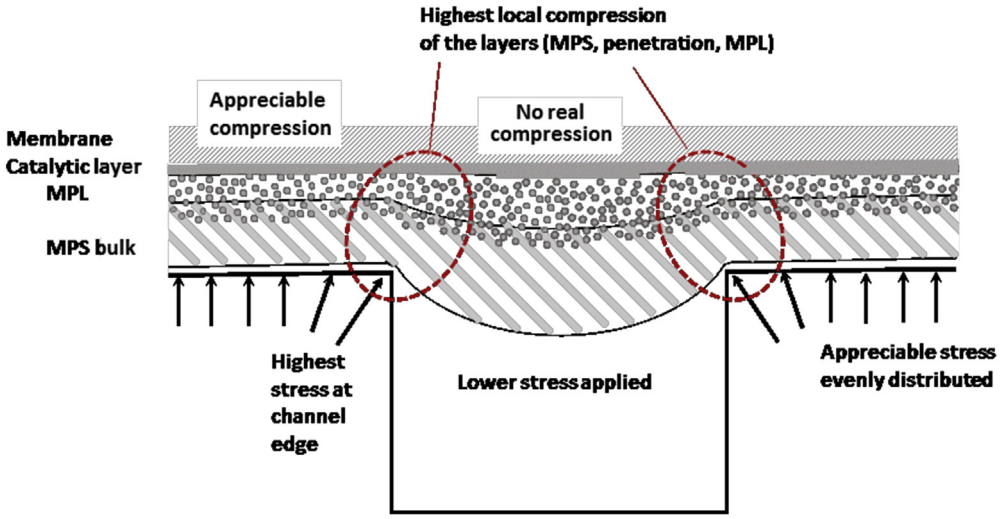

Fig. 4. Localized compression of the GDL in a fuel cell caused by the grooved channels in bipolar plates. For the sake of simplicity, only one compartment is shown.

of GDLs: according to [97], paper-type GDLs are more sensitive than felts or cloths.

Because of the importance of this phenomenon, solutions for mitigation have often been searched using ex-situ techniques, allowing a large number of freeze-thaw cycles to be carried out. For instance Lee and Mérida [95] designed a dummy fuel cell, i.e. without the membrane-electrode assembly: in this cell, the rear side of the MPS was in contact with one bipolar plate, whereas the MPL external side faced the second bipolar plate. Performing more than 50 cycles, with air circulation between −35 °C and 20 °C in the cell did not result in visible strain or change in porosity, surface angle, bending stiffness and through-plane resistivity. On the contrary through-plane and in-plane permeability values were significantly enhanced which indicated a loss of material from the GDL structure induced by air circulation (this aspect will be described in the following sub-section).

It has to be mentioned that in most papers dealing with freezing-thawing conditions, very little concern is put on MPLs: it is likely that the MPL does not directly suffer from such harsh operating conditions, in spite of the above delamination. In particular, in the often encountered case of deposited MPL on the macroporous substrate, because of the presence of intermediate layer between the MPS and MPL bulk, consisting of micrometric carbon particles onto far larger entities forming the MPS in a three dimensional structure, it is likely that the adhesion of the MPL on MPS is less affected than that on the catalytic layer. However, the presence of MPL may be no great help to mitigate freezing-thawing conditions, even though it hinders intrusion of carbon fibres into the catalytic layers as reported by Ref. [98]. Moreover in some cases, the presence of MPL can be detrimental to the catalytic layer because of the larger amount of water in the catalytic layer and in the membrane even after the operation [99] – even though MPLs are designed to allow easier water evacuation to the MPS. According to the authors, the loss of mass transport rate upon freeze-thaw cycles is delayed by the presence of the MPL but without exhibiting a terminal degradation state.

4.3. Erosion by fluid circulation

4.3.1. Gas circulation

The velocity of the gas in the channels of the bipolar plate can attain very high values. For instance, consider a bipolar plate of a 100 cm^2 cell, with ten parallel channels having a 1 mm^2 cross-section. Running the cell at 1 A cm^{-2}, with air fed with a stoichiometric factor of air oxygen λ at 2, results in a velocity in the order of 6 m s^{-1}. Gases are continuously circulated in the bipolar plate: in contact with the rough surface of the MPS, friction phenomena are to occur, in particular in the presence of liquid water: in addition to the local effects of the compression, friction phenomena are known to induce appreciable erosion of the carbon-based material [100,101]. This effect is more pronounced at the cathode side than near the anode because of very different flow rates of air and hydrogen under regular conditions. Erosion and loss of hydrophobicity can appear after 150 h operation [5].

Investigation of this degradation phenomenon is usually carried out in accelerated stress tests using a dummy cell without electrodes, but with the membrane inserted between the two GDLs investigated. The cell compartments are fed with heated, humidified air with a stoichiometric factor usually far larger than that employed in regular fuel cell operation, corresponding to gas velocity in the channels in the order of 20–50 m s^{-1}. After a given period of time, the cell is dismantled and the aged GDL is inserted in a regular fuel cell, for conventional electrochemical characterization and assessment of their degradation during the test. The nature and the significance of these degradation phenomena are commented below.

As a matter of fact the loss of hydrophobicity is linked to erosion, i.e. to the loss of material caused by the friction of the circulating air on the surface. Because of the small dimensions of the channel, the pressure at the surface – called shear stress τ – in particular on a protruding defect can be very high and cause the detachment of particles from the GDL surface, creating then a cavity. Because of the low compactness and the moderate mechanical resistance of GDL materials, erosion becomes gradually more significant. To illustrate this point, the shear stress in the above fuel operated at 1 A cm^{-2}, has been calculated depending on the number of channels in the plate and the stoichiometric factor of dry air circulating at 80 °C. Usual correlations for pressure drop have been taken for this purpose, and for the sake of simplicity, the gas ducts have been considered cylindrical for easier estimation of pressure drop, from which shear stress values could be calculated. As shown in Fig. 5, reducing the number of channels forces the gas to higher velocity in the flow pattern, resulting in higher τ values. Moreover, these estimations show the effects of AST, with λ factors usually larger than 5, in comparison with the values for regular operation, typically ranging from 2 to 3. Whereas the sides of the channel do not suffer

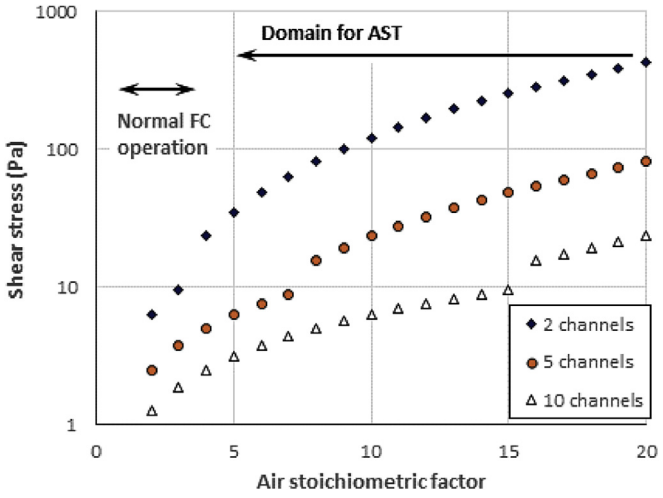

Fig. 5. Variations of the shear stress with the stoichiometric factor of air oxygen and the number of parallel channels in the flow pattern.

from high speed flow, the irregular surface of the MPS is to be more prone to erosion. However, this does not provide an explanation for the degradation at the MPL, which is not directly facing the high gas circulation rate.

Chun et al. [100] performed such tests using a single commercial SGL 10 BC with a large excess of hot dry air ($\lambda = 20$) for 14 days (336 h): no cracks on the MPL surface were observed after the long runs. After this first period, the air feed was fully humidified, which resulted in the formation of the first cracks from day 15, with formation of puddle-shaped defects around the cracks, for possible water accumulation. Characterization of the GDL after day 28 (i.e. after 14 days upon humidified gases) revealed very little weight loss together with the reduction in F-containing species in the GDL bulk and contact angle; the cell voltage under regular operation was decreased only at high current density (cd) which may be related to poorer water management. Because of too strong adhesion of the GDL with the membrane during these AST, the technique has been improved by Wu et al. [102] by insertion of perforated polyimide films and a thin MPL layer on the Nafion sheet. Air and hydrogen at high stoichiometric factors were saturated with vapour at 80 °C then heated up to 120 °C before flowing in the dummy cell for 200 h: reduction in the cell voltage was afterward observed mainly at high current density. Tests with pre-aged GDL by regular fuel cell operation or hot pressing at high temperatures, led to far larger effects of the 200-h long AST. An interesting point mentioned by the authors is that the loss of hydrophobicity in the GDL bulk, although being detrimental to water management, has a positive effect on the electrical conductivity of the layer, expressed by a lower ohmic resistance of the overall cell.

Improvement of GDL design and preparation has been the topic of various investigations in view to increased durability, e.g. by addition of a polymer binder to the MPL ink [100]: whereas cracks in the MPL surface were formed during the drying period at 350 °C, the binder, although decomposing in this period, allowed better internal cohesion of the fine carbon particles in this layer, resulting in a crack-free surface. This improved MPL deposited on a conventional MPS was observed to resist to the above 14 day-AST with humidified gases with no visible change of the MPL surface and insignificant decrease in the cell performance. Another technique consists in partial replacement of carbon black particles by carbon nanotubes (CNT) in the ink [101]: with 10% CNT in the carbon charge, both performance and durability of the lab fuel cell were shown to be improved by the substitution. In spite of the presence of CNT, severe cracks were observed on the surface of the improved MPL after 1000 h-long circulation of hot humidified air. In addition the cell performance was significantly reduced, mainly at high current density, e.g. with a cell voltage nearly 160 mV lower at 1.24 A cm^{-2}, whereas the ohmic and mass transfer resistances at this current density were increased by approx. 50 and 100% respectively. Weight loss of the overall GDL attained 20% and the contact angle was reduced by nearly 10°. Comparison with other erosion AST data is difficult because of the very long period of time considered in this study.

To conclude, fluid dynamics can partly explain the degradation induced by high rate gas circulation at the MPS side. Nevertheless the presence of water vapour and the elevated temperature is likely to exert a synergetic action by thermal and possibly chemical mechanisms, resulting in appreciable MPL degradation.

4.3.2. Forced circulation of water

In order to better understand water management and flow of liquid water in fuel cells, Kandlikar et al. [89,103] performed AST with forced circulation of water through the GDL in a dummy cell described in Ref. [104] and operated at 80 °C, 14 bars, with a water flow rate corresponding to that produced at the cathode at 2 A cm^{-2} for 500 h. As a matter of fact, the forced convection of hot water induces leaching of water-repellent agents from the GDL, as observed by the changes in the contact angle on the MPL surface, and the profiles of the dynamic capillary pressure, for which the voltage fluctuations exhibited far smaller peaks at the end of the run, corresponding to easier passage of water through the dual carbon layer.

The phenomenon leaching has been mentioned above but is discussed at greater length in the following section.

5. Physicochemical degradation of GDLs

Physicochemical degradation can be classified under (i) chemical dissolution in solutions, being oxidant or not, and (ii) electrochemical dissolution. In all cases the aged GDL samples are submitted to various characterization tests for assessment of their intrinsic properties or their behaviour in a FC under operation. Investigation of these degradation phenomena can be aimed at evaluating the durability of GDL component, but also at better understanding of the role of the GDL in the cell, in both its performance and its durability: how does the GDL contribute to improve this durability, and in particular what is the specific role of the MPL?

5.1. Chemical dissolution in solutions

Tests usually consist in soaking GDL samples in pure water [67,105,106] or in 10–20 wt% acidic solutions [22,75,101,107]: the ex-situ test is performed for 1000 or 2000 h at high temperatures, for the sake of more aggressive conditions as usual. The use of sulfuric acid at appreciable concentration corresponds to the same purpose, i.e. to magnify greatly the acidic conditions reigning in a cell under operation. The presence of acid in the liquid is often considered as enhancing the degradation extent in comparison with pure water. In some papers, air sparging is continuously used in the tests, whereas other investigations have been carried out without circulation of the gas: presumably the presence of oxygen in the liquid amplifies dissolution processes.

5.1.1. Visual aspect of the degradation and evidence of loss of hydrophobicity

Loss of material caused by the AST is first evidenced by weighing the GDL sample before and after the AST: SEM observation of the

GDL surface is usually conducted on both faces for more precise description of the dissolution. After the ageing test in a sulfuric solution, the carbon filler and the graphitized resins added to the MPS have been reported to have undergone visible degradation.

As shown in Fig. 6b for the example of 24 BC GDL, the MPL surface observed under high magnification after the 1000 h-long test, is slightly less compact than that of the pristine MPL (Fig. 6a), with the presence of micrometric cavities, faults and breaks (Fig. 6b) caused by partial dissolution of the graphitized resins. Mesoscopic morphology of the MPL surface longer discussed in section 5.2, is not visibly affected by immersion tests (data not shown). Fresh MPS surface (Fig. 6c) shows the presence of graphitized resins and the carbon-based fillers protecting efficiently the mesh of carbon fibres. Immersion in hot sulfuric solutions of 24 BC GDL results in severe decomposition of the protecting resins, with partial dissolution of the filler, so the surface of the MPS fibres appears nearly bare after the treatment (Fig. 6d). Surprisingly, similar treatment of 24 BA GDL (without MPL) seems less detrimental to the surface of the MPS structure, with less significant dissolution of the resins and little visible dissolution of the filler between the fibres (Fig. 6e). For such treatments, deposition of the MPL onto the MPS surface is not necessarily better, at least for the durability of the GDL.

The loss of hydrophobicity is directly expressed by the reduction in the contact angle of the surface by the treatment. The contact angle is observed to decrease by 5–15° in the course of the treatments depending on the GDL material and the operating conditions. The presence of the MPL appears significant for the protection of the substrate as shown by contact angle measurements [1,22,105]. Moreover, the amount of PTFE in the MPL, up to 23% was observed to be essential to mitigate the loss of hydrophobicity of this surface [105].

5.1.2. *Cause of the loss of hydrophobicity upon immersion*

This loss is sometimes attributed to the loss of F-containing compounds in both the MPS and the MPL structures [67,105,108], but other contributions [22,106] showed that the phenomenon was principally due to dissolution of the carbonized or graphitized materials, accompanied by detachment of carbon particles from the structure, which becomes more porous. Chemical and spectroscopic analysis are generally employed to highlight the nature of the overall degradation.

IR analysis of the ageing sulfuric solution indicates the presence of C–F bonds [75]. This fact could be confirmed by TGA measurements: the weight loss observed between 550 and 620 °C usually attributed to thermal decomposition of F-based compounds, was found to be slightly lower in the aged GDL than in the fresh materials. However, in other comparable investigations, the change in weight loss in the TGA runs are described as of little significance [22,106], corresponding to negligible dissolution of F-containing compounds in the AST. This fact has been demonstrated by additional test with F-free MPS without MPL: the loss of hydrophobicity of this material was revealed to be even more significant than with the regular F-containing (MPS-MPL) combination.

XPS analysis of the GDL surface is often used for both qualitative and quantitative identification of the chemical groups and bonds. As observed in previous works, for the case of 24 BC-like GDLs prepared in CEA [107], long term immersion in sulfuric solution led to formation of O – containing groups on both MPL and MPS surfaces as shown in Fig. 7. The action of hot water is usually far less significant. Contrary to Yu et al. observations [75], the concentration of F atoms on the surface was not significantly changed by the AST. However, more precise examinations of the XPS spectra led to more precise information on the chemical changes induced by the treatment (Fig. 7). First, carbon atoms of MPS and MPL surface are oxidized to C=O groups upon immersion in the two liquids, with formation of C–O bonds in the case of the acidic solutions (Fig. 7); formation of C–O appears more significant on the MPS surface (Fig. 7, bottom). Secondly, F groups are mainly in the form of CF_2 on the fresh MPL (Fig. 7, top) and more probably in the form of [CF_x-CH_y] for the fresh MPS (Fig. 7, bottom). Whereas immersion in hot water did not change the nature of the F-containing groups on the surface (data not shown), treatment in acidic solution was found to be stronger at the MPL for which the native CF_2 groups are significantly transformed to [CF_x-CH_y] groups (Fig. 7, top).

The cause of the loss of hydrophobicity still appears

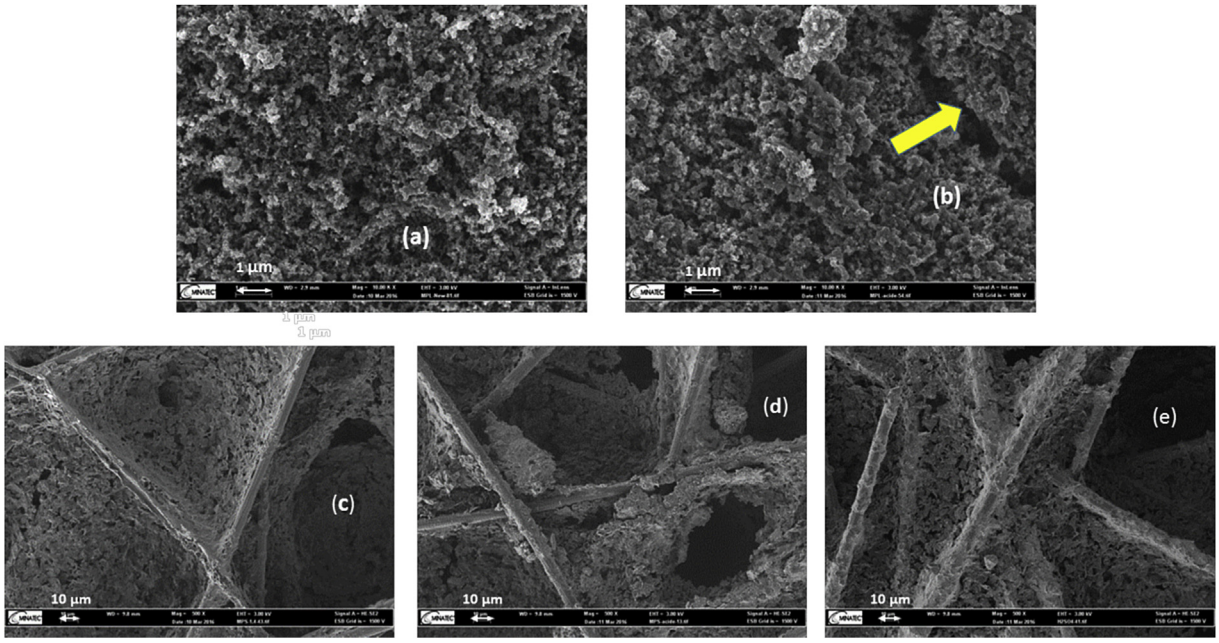

Fig. 6. SEM views of 24 BA and 24 BC Sigracet GD, with effect of 1000 h immersion in 10 wt% sulfuric solution at 80 °C: (a) MPL side of the pristine 24 BC; (b) same view after the treatment; the arrow indicates the presence of a crack; (c) MPS view of the pristine 24 BC; (d) MPS view of the aged 24 BC; (e) MPS view of the aged 24 BA (no MPL).

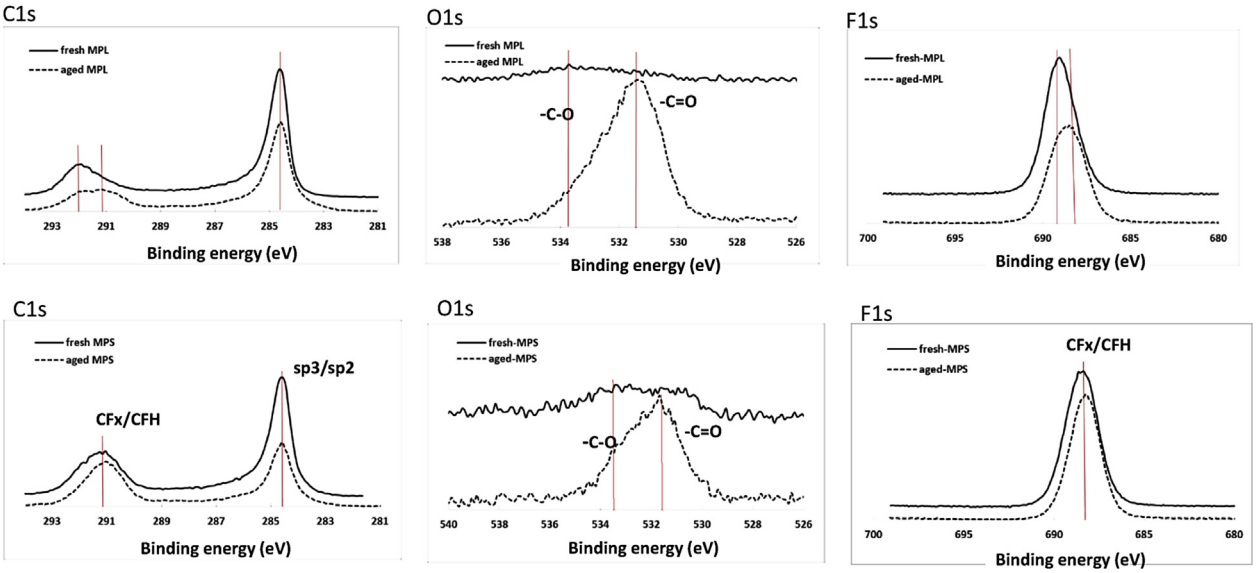

Fig. 7. XPS measurements on GDL surfaces before and after 1000 h immersion in 10 wt% sulfuric acid at 80 °C. Top: MPL surfaces; bottom: MPS surfaces.

controversial. However, it can be concluded from a closer analysis of the data reported that F loss by dissolution probably occurs but to a small extent, being sometimes observable, sometimes hidden by the accuracy of the measurement. More probably, the carbon surface is partly oxidized to O-containing compounds as shown by the above mentioned XPS data: this is not in contradiction with the partial dissolution of the carbonaceous resin reported by the Korean group [22,106] and the detachment of carbon matter. The relative significance of F loss in comparison to oxygenated compounds is probably dependent on the nature of the GDL employed, data which is unfortunately not given in all contributions.

5.1.3. Effect on the cell performance

This change in GDL surface is usually accompanied by change in the electrochemical performance: the voltage vs. current density curves with the aged GDL usually deviates from that with pristine GDL, in particular at high current density, e.g. with reduced cell voltage by approx. 100 mV at 1.24 A cm^{-2} [101]. Moreover, this decrease in cell performance is more visible with fully humidified gases, which can induce more troublesome transport phenomena in the MEA structure: in such case water is less efficiently removed from the MPL at the vicinity of the catalyst layer. More sluggish transport phenomena have been confirmed by EIS, with a 60% increase in the diffusion resistance after 1000 h immersion in sulfuric solution. Interestingly, Cho et al. [106] observed the voltage transient of the fuel cell submitted to current steps from 0.6 to 1.2 A cm^{-2} or vice versa, depending on the relative humidity RH and the stoichiometric factor of inlet air, λ. For the higher current density, RH = 100% and low λ values, the cell voltage is subjected to fluctuations: these fluctuations are greatly amplified in the cell provided with the aged GDL and are visible even with large excess of atmospheric oxygen. For lower humidification of air (RH = 50%), fluctuations of the cell voltage are still visible at low λ values. Besides, sudden increase in the current is accompanied by a (negative) overshoot of the cell voltage which has been attributed by the authors to a transient dehydration of the membrane, which is rapidly compensated by the increased production of water. At high current density, the degraded structure of the GDL allows the formation of "puddle water lakes" between the macropores initially present in the structure [106]: liquid water is then retained in the MPS, which is then more prone to flooding.

Another consequence of the loss of hydrophobicity mentioned by Lattorata et al. is the increase in the ohmic resistance, which might be due to looser mechanical and less efficient electrical contact between the GDL and the other cell components.

5.1.4. Use of oxidizing solutions

As a matter of fact, the presence of air sparging in the hot liquids can be considered as an example of oxidizing conditions, in spite of the moderate solubility of oxygen in aqueous media at 80 °C. Stronger aggressive conditions can be studied with 30% hydrogen peroxide solutions [96,107,108]. Hydrogen peroxide can actually be formed as the intermediate species in the reduction of oxygen, but is also formed in by chemical combination of oxygen diffusing through the membrane to hydrogen [1,3]. Tests are conducted for shorter periods of time than upon immersion in simple sulfuric solutions. The conclusions reported are far less abundant and more briefly commented in comparison to the effect of other physico-chemical stresses induced. They do not differ significantly from each other: lower performance of the cell at high current density and loss of hydrophobicity have been also reported. Nevertheless, the cause of this loss – dissolution of hydrophobic graphitized resins or degradation of the F-containing polymers has never been documented.

Fenton agent prepared by addition of Fe^{2+} cations at ppm levels into hydrogen peroxide leads to formation of OH radicals, which are known to be formed in fuel cells upon side diffusion of oxygen and in the presence of traces of transition metal cations: this is representative of real situations for instance with stainless steel bipolar plates – and their insufficient surface treatment – or the balance of plant (BoP) components. This agent used for investigation of other fuel cell components [109], seems to have never been employed for GDL investigations up to now.

5.2. Electrochemical degradation

GDLs consist mainly of carbon-based materials, so degradation in the cathode side may primarily be considered as being source of carbon corrosion/oxidation. Three reactions can occur at carbon materials, then in fuel cell GDLs as follows:

$$C + 2\,H_2O = CO_2 + 4\,H^+ + 4e \quad E_0 = 0.207\ V/NHE$$

$C + H_2O = CO + 2\ H^+ + 2e\ E_0 = 0.518$ V/NHE

$CO + H_2O = CO_2 + 2\ H^+ + 2e\ E_0 = -0.103$ V/NHE

Direct combustion of carbon is known to have sluggish kinetics. However, the presence of metal cations e.g. Pt^{2+} cations generated by CL ageing can catalyse the reaction to some extent. Whereas corrosion from the catalyst layer can be observed from 0.7 V, the presence of more inert materials e.g. graphitized resins together with fluorinated polymers covering the structure surface is thought to inhibit additional corrosion of the GDL. However, because of the composite structure of GDL, with or without MPL, preferential sites for corrosion – with lower protection – are first prone to dissolution: the materials removed create more space for further corrosion, resulting in growing importance in oxidative dissolution. Moreover, direct cleavage of fluorine-carbon bonds cannot occur at potentials compatible with fuel cell operation (in contrast, OH radicals produced through indirect pathways can degrade such "inert polymers").

For AST, it is often preferred to submit the cathode to high positive potentials to magnify the degradation effect, but also to mimick the very high cell voltage in the transient period of fuel cell start-up, where hydrogen is suddenly introduced into the anode chamber [110,111].

This large domain of degradation techniques reviewed for instance in Ref. [66], can be separated into ex-situ and in-situ tests.

a) Ex-situ electrochemical tests

The GDL is placed in an electrolytic cell and acts as the working electrode: immersed in a dilute sulfuric solution, the GDL is submitted to high positive potentials referred to the reference electrode. Depending on the literature source, the GDL potential varied between 1 and 1.45 V/SCE, i.e. nearly 1.25–1.7 V/NHE, which actually represents very positive potentials, comparable to the standard potentials of strong redox couples i.e. Ce (III)/Ce (IV) or even Ag (I)/Ag (II) at 1.45 or 1.82 V/NHE respectively. A first comment to be made is that, in most published works, a high potential has been applied to the GDL for periods of time in the order of 100 h, sometimes with regular assessment of the degradation extent. With exception of ref. [112], no indication on the anode current at the aged GDL is given, so the amount of matter dissolved – assuming for instance that only carbons dissolves – cannot actually be estimated. It is often assumed that only carbon dissolves in the ageing process [69,112]. From the data reported in Ref. [112], the carbon loss in the 96 h ageing run varied approx. from 20 to 420 μg cm^{-2} as the GDL potential varied from 1 to 1.4 V/SCE: from the initial carbon powder loading, up to 25% of the MPL was dissolved in the ageing test. Engineers may regret that too little information on the current passed in these tests be given for simple but quantitative evaluation of corrosion significance.

According to most authors, electrochemical corrosion concerns mainly the MPL: more precisely, using GDLs with different penetration depths of the MPL, Cho et al. [63] showed that the most corroded part of the GDL was the penetrating portion of the MPL, with dissolution of the fillers and the carbon particles introduced. The observations reported in Ref. [69] fully support this phenomenon. Electrochemical corrosion induces the formation of macropores in the MPL, the increase in mean asperity and the reduction in mechanical cohesion between the MPS carbon fibres [112]. The loss of hydrophobicity resulting from the dissolution, favours liquid water retention in the MPL [63,69]. As a matter of fact, as clearly illustrated in Ref. [63], the main difference between chemical and electrochemical stresses is the region where liquid water can accumulate (see above section): in the MPS after chemical dissolution, and in the MPL penetration volume at high potentials. At the mesoscopic level, the effect of high polarization on MPL can be observed in Fig. 8, with the formation of mesoscale cracks on the MPL surface of a commercial 24 BC GDL. Although the surface of fresh 24 BC materials exhibits long cracks approx. 10 μm broad, that have been probably caused by the manufacture process: the defects appear neatly defined and the zones between the cracks are of high compactness (Fig. 8a). After 96 h ageing at 1.4 V, the large cracks existing in the fresh materials are still visible but somewhat broader (Fig. 8b): corrosion likely occurred in the sides of the "original" cracks. Besides, secondary cracks of lower width and lengths have been formed in the ageing run, resulting in a better-developed defect network on the overall surface. As reported by Chen et al. [112], degradation of MPL surfaces is visible only for potentials larger or equal to 1.2 V/SCE.

As matter of fact, MPS are also affected by electrochemical degradation [23,112]: appreciable thinning of the carbon fibres and change in the substrate morphology, in particular by debonding of the fibres from the matrix [23] – principally caused by dissolution of the resins. Paper MPS undergo lower weight reduction that carbon cloths, because of the high temperature treatment in their manufacture but suffer more than cloths from the degradation of internal structure.

The loss of hydrophobicity evidenced by contact angle measurements corresponds to the loss of the hydrophobic agent from the surface. Two interpretations are usually expressed in literature either the loss of fluoride in the overall component, or the oxidation

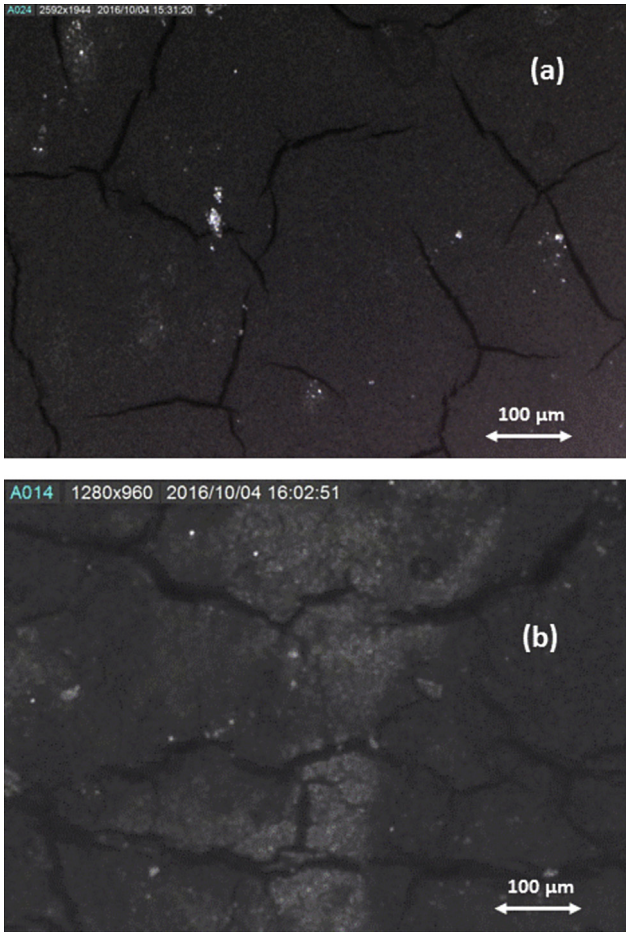

Fig. 8. View of the MPL surface of 24 BC GDL before ageing (a), and after 96 h at 1.4 V/SCE (b).

of the graphitized resins: increased formation of carboxyl and hydroxyl groups and even dissolution of the resins. According to [112], dissolution of F-containing polymers is little significant in comparison to carbon-based materials. However, TGA measurements and XPS revealed the loss of F elements from the GDL. This is also accompanied by conversion of CF_2 groups of MPL surfaces to [CF_x-CH_y] groups in addition to the formation of ethers, alcohols and carbonyl functions [69].

b) In-situ electrochemical tests

Because tests are conducted using fully mounted fuel cells, all components are submitted to the stress applied, in particular the catalytic layer and the GDL. When observing the consequences of the stress, one difficulty to be solved is to distinguish the response of the CL from that of the gas diffusion layer, as often expressed in the literature. Substitution of one component by another can be considered for this purpose as follows:

- After recording the overall corrosion of C from the catalytic layer and the GDL by measurement of the amount of CO_2 emitted, replacement of the carbon-supported CL by non-supported catalyst and performing similar measurement, can yield the contribution from the GDL [44,105].
- After the evaluation of the state of health of the cell by recording the variations of the cell voltage with the current density, one aged component is replaced by a fresh one: through interpretation of the responses obtained by fitting the experimental voltage vs. cd variations to the mathematical law derived from the expression of the various overpotentials, Aoki et al. [108] could deduce qualitatively the contribution of the GDL in the degradation upon high cell voltage.

5.2.1. In-situ degradation at high potentials

For the present case of GDLs, the AST employed may differ from the usual standards established by the DOE or comparable organisations, for catalytic layers or the membrane [2]. Usually the cell is fed with hydrogen and nitrogen and the cell voltage is fixed at 1 V or more for given periods of time. The degradation extent can be evaluated from the V vs. cd variations – from the reduction in limiting current density allowed by the fuel cell [105,109], or by the decay of the ECSA along time [44]. Generally speaking, the catalytic layer suffers much more from the AST than the GDL, with significantly greater amounts of carbon corroded, as reported in numerous papers [44,105,108]. Corrosion of the carbon in the CL can be detrimental to the electrode activity, as non-supported Pt particles are to be lost, and to gas diffusion transport toward the catalytic sites. In the GDL, the corrosion affects only the efficiency of gas transport from the channel to the catalytic layer. Aoki et al. [108] could show that the increase in the diffusion overpotential in the cell under operation was mainly due to carbon loss from the catalytic layer. The GDL is actually altered in the AST, by both carbon corrosion and loss of its hydrophobicity. This phenomenon is accelerated at higher temperatures and upon high humidification of the gases [105]. NB. In comparison with literature published with dissolution AST or ex-situ electrochemical degradation, the question on whether the change in hydrophobicity is caused by the loss of F-containing polymers or carbon-based materials, is rarely discussed.

The role of MPL on the resistance of the cell components to high potentials has been evidenced in Ref. [44]. First, in the first hours of AST at 1.2 V, the ECSA decay of the electrode was not found to be affected by the presence of the MPL; after 7 h, contrary to what was observed with the simple MPS (SGL 24 BA), the presence of an MPL limited the decrease in ECSA. In addition, the increase in Pt particle size caused by Oswald ripening is less significant with a GDL provided with an MPL. The two facts confirm the protective role exerted by the MPL on the catalytic layer, as indicated by the higher cell voltage measured at low current density. Thinning of the CL was also shown to be reduced by the MPL between the mesoporous C structure and the large carbon fibres of the MPS. In addition cell voltage at high current density is far larger with the MPL, corresponding to protection of both the CL and MPS structure in the AST. The presence of an MPL in the cell has been shown by Spernjak et al. to affect the cd distribution at fixed average cd along the AST [44]: with the MPL, the current distribution turns to be more uneven which can be described in terms of two apparent zones in the cell: the region closer to the inlet with a high current density, whereas the current density is far lower in the outlet region, expressing presumably more significant degradation of the cell component due to flooding.

5.2.2. Degradation in fuel cell under real operation

In such cases, the entire fuel cell is submitted to the ageing test with production of electricity: as expressed in relevant reviews [1,3,66]. These tests can consist in long-term runs at nominal conditions or in standard cycling tests [113], or for instance with the New European Driving Cycle (NEDC) suitable to mimick urban driving conditions [114,115], or by cycling the current density or the potential between two very different levels, cycling the relative humidity of the inlet gases [116] etc. For the evaluation of the state of health of the cell, the changes induced to the GDL can be determined and quantified by using electrochemical techniques (see Section 3).

The conclusions expressed by the related literature are far less abundant in terms of comprehensive information, probably because durability tests in real conditions (long-term tests at nominal cd or under cyclic conditions) have often been conducted for evaluation of a novel component design or technology. The information reported is usually in accordance with the conclusions expressed from more dedicated tests (ex-situ or in situ in H_2/N_2 conditions), with comparable description of phenomena and interpretation.

6. Conclusion and routes for improved durability

For the last decade, impressive progress has been achieved for higher durability of membrane fuel cells through more efficient design of the gas diffusion layers, in particular through optimal design of microporous layers. As expressed indirectly from this contribution, the improvement in MPL design and formulation can be facilitated by thorough understanding of degradation phenomena in the gas diffusion layers, in relation to the other neighbouring components, namely the electrodes and the distribution plates.

Current pathways for improvement of both the performance and durability of the cell – regardless of the membrane and the catalytic layer – can be allowed by the use of more sophisticated carbon particles in the MPL structure such as carbon nanotubes, in spite of their cost. Moreover, the concept of MPL may totally differ from that of porous carbon-based layers, for the sake of reduced corrosion. For instance MPL can be formed by deposition of porous titanium, as expressed in Section 2, or by adding antimony doped tin oxide to conventional Vulcan XC-72 [117], or based on silicon carbide [118]. Whereas carbon based materials have usually been considered as the continuous phase of the GDL, with possible addition of suspended other particles, it has also recently be considered to design a fluorine-containing continuous phase (F-functionalised polyvinylidene) filled with graphite and carbon black particles acting as the conductive phase: the resulting

material exhibits higher adhesion with the catalyst layer [119].

In addition, gradient of hydrophobicity in the GDL has been suggested for a couple of years with insertion of several MPLs of various hydrophobicity levels [4,120–122], for more efficient management of water, which is also to contribute to GDL durability: the overall strategy to be adopted still appears controversial (should the hydrophobicity variation between the distribution plate and the CL be monotonic or exhibit a maximum?) but the approach of Cho's group relying on the estimation of capillary gradients is to bring the final answer depending on the MPS and MPL component properties. Besides, hydrophobicity gradient can also be engineered along the fuel cell plane: for this purpose, recent advances in surface modification by grafting diazonium groups [36] or by functionalization by N- or O- groups [123] after irradiation allow spatially distributed hydrophobicity of the MPL: as a matter of fact, because the water amount usually increases from the inlet to the outlet, it might be imagined that GDL has to be more hydrophobic near the outlet of the cell than in the inlet section. This strategy is currently under investigation in our labs.

Another parameter of the MPL design is its thickness in relation to that of the MPS [17,124] and its penetration depth, as discussed in Ref. [63].

These strategies, some of them being highly sophisticated, are to improve the performance of the cell. Nevertheless, upon long-term operation under residential or urban transport cycles, the various components are affected in their dimensions as well in their physicochemical properties. Scientists and engineers have to remain aware of this quasi inevitable fact, which can sometimes render inapplicable an advanced technology because of its too high sensitivity to operating parameters. One solution that could be suggested – although more difficult to achieve – is to design components, here MPS and MPL, in a way that their change over time for the targeted application does not affect too much their ability and the overall cell performance. For this purpose and also because GDLs have to be an acceptable cost – near 4 $/m^2 according the DOE target for 2015 -, robustness would be favoured. It might nevertheless be suggested to select the MPS and MPL materials depending on the membrane properties and the catalyst support, for optimal combination in the designed fuel cell.

Acknowledgments

This work has been carried out within the CEATech program in France, with the active contribution of Région Lorraine in particular for M. Belhadj's PhD grant.

References

[1] R. Borup, J. Meyers, B. Pivovar, Y.S. Kim, R. Mukundan, N. Garland, D. Myers, M. Wilson, F. Garzon, D. Wood, P. Zelenay, K. More, K. Stroh, T. Zawodzinski, J. Boncella, J.E. McGrath, M. Inaba, K. Miyatake, M. Hori, K. Ota, Z. Ogumi, S. Miyata, A. Nishikata, Z. Siroma, Y. Uchimoto, K. Yasuda, K.-I. Kimijima, N. Iwashita, Chem. Rev. 107 (2007) 3904–3951.
[2] S.-S. Zhang, X.-Z. Yuan, H.-J. Wang, W. Merida, H. Zhu, J. Shen, S.-H. Wu, J.-J. Zhang, Int. J. Hydrog. Energy 34 (2009) 388–404.
[3] F. Lapicque, C. Bonnet, B.T. Huang, Y. Chatillon, Analysis and evaluation of ageing phenomena in PEMFCs, in: K. Sundmacher (Ed.), Advances in Chemical Engineering, Fuel Cell Engineering, vol. 41, Academic Press, New York, 2012.
[4] L. Cindrella, A.M. Kannan, J.F. Lin, K. Saminathan, Y. Ho, C.W. Lin, J. Wertz, J. Power Sources 194 (2009) 146–160.
[5] A. El-Kharouf, B.G. Pollet, Gas diffusion media and their degradation, in: M.M. Mench, E.C. Kumber, T.N. Verziroglu (Eds.), Polymer Electrolyte Fuel Cell Degradation, Academic Press, New-York, 2012, pp. 215–247.
[6] J. Park, H.-Y. Oh, T. Ha, Y.I. Lee, K.-D. Min, Appl. Energy 155 (2015) 866–880.
[7] M. Watanabe, M. Tomikawa, S. Motoo, J. Electroanal. Chem. 182 (1985) 193–196.
[8] S.B. Park, J.-W. Lee, B.N. Popov, J. Power Sources 163 (2006) 357–363.
[9] K. Karan, H. Atiyeh, A. Phoenix, E. Halliop, J. Pharoah, B. Peppley, Electrochem. Solid-State Lett. 10 (2007) B34–B38.
[10] Z.-G. Qi, A. Kaufman, J. Power Sources 109 (2002) 38–44.
[11] G.G. Park, Y.J. Sohn, T.H. Yang, H.G. Yoon, J.-W. Lee, C.-S. Kim, J. Power Sources 131 (2004) 182–187.
[12] W.-M. Yan, C.-Y. Hsueh Soong, F.-L. Chen, C.-H. Cheng, S.-C. Mei, Int. J. Hydrog. Energy 32 (2007) 4452–4458.
[13] S. Kundu, K. Karan, M. Fowler, L.C. Simon, B. Peppley, E. Halliop, J. Power Sources 179 (2008) 693–699.
[14] V.A. Paganin, E.A. Ticianelli, E.R. Gonzales, J. Appl. Electrochem. 26 (1996) 297–304.
[15] L. Giorgi, L. Antolini, A. Pozio, E. Passalacqua, Electrochim. Acta 43 (1998) 3675–3680.
[16] M. Han, S.H. Chan, S.P. Jiang, J. Power Sources 159 (2006) 1005–1014.
[17] S.B. Park, J.-W. Lee, B.N. Popov, Int. J. Hydrogen Energy 37 (2012) 5850–5865.
[18] T.Y. Kim, S.J. Lee, H.Y. Park, Int. J. Hydrog. Energy 35 (2010) 8631–8643.
[19] A.Z. Weber, J.S. Newman, J. Electrochem. Soc. 152 (2005) A677–A688.
[20] R. Schweiss, Fuel Cells 16 (2016) 100–106.
[21] J.H. Nam, K.J. Lee, G.S. Hwang, C.J. Kim, M. Kaviany, Int. J. Heat. Mass Trans. 52 (2009) 2779–2791.
[22] T. Ha, J. Cho, J. Park, K. Min, H.-S. Kim, E. Lee, J.-Y. Jyoung, Int. J. Hydrog. Energy 36 (2011) 12427–12435.
[23] R.J.F. Kumar, V. Radhakrishnan, P. Haridoss, Int. J. Hydrogen Energy 36 (2011) 7207–7211.
[24] A. Rofaiel, J.S. Ellis, P.R. Challa, A. Bazylak, J. Power Sources 201 (2012) 219–225.
[25] M. Inoue. Carbon fibre paper for solid polymer fuel cells, US Patent US6489051B1 (2002).
[26] M. Nakamura, Y. Hosako, H. Ohashi, M. Hamada, K. Mihara, Porous carbon electrode substrate and its production method and carbon fibre paper – US Patent US7297445B2 (2007).
[27] K. Jorder, W. Schafer, H. Rettig, K. Salama, A. Bock, S. Wagener, A. Helmbold, Conductive nonvowen – US Patent US2003/0109189 A1 (2003).
[28] A. Jayakumar, S.P. Sethu, M. Ramos, J. Robertson, A. El-Jumaily, Ionics 21 (2015) 1–18.
[29] M. Mathias, J. Roth, J. Fleming, W. Lehnert, Chapter 46, Diffusion Media Materials and Characterization. Handbook of Fuel Cells, Fundamentals, Technology and Applications, in: Fuel Cell Technology and Applications, vol. 3, John Wiley & Sons, Ltd., 2003.
[30] L. Caramaro, Textiles à usage technique, Techniques de l'Ingénieur, 2006. N2511 [in French].
[31] H. Ito, K. Abe, M. Ishida, A. Nakano, T. Maeda, Munakata, H. Nakajima, T. Kitahara, J. Power Sources 248 (2014) 822–830.
[32] G.R. Molaeimanesh, M.H. Akbari, Int. J. Hydrogen Energy 39 (2014) 8401–8409.
[33] C. Lim, C.Y. Wang, Electrochim. Acta 49 (2004) 4149–4156.
[34] P. Gallo Stampino, S. Latorrata, D. Molina, S. Turri, M. Levi, G. Dotelli, Solid State Ionics 216 (2012) 100–104.
[35] Y. Hiramitsu, H. Sato, K. Kobayashi, M. Hori, J. Power Sources 196 (2011) 5453–5469.
[36] Y.R.J. Thomas, A. Benayad, M. Schroder, A. Morin, J. Pauchet, ACS Appl. Mater. Interfaces 7 (2015) 15068–15077.
[37] C.-J. Tseng, B.T. Tsai, Z.-S. Liu, T.-C. Cheng, W.-C. Chang, S.-K. Lo, Energy Conv. Manag. 62 (2012) 14–21.
[38] H. Choi, O.-H. Kim, M. Kim, H. Choe, Y._H. Cho, Y.-E. Sung, ACS Appl. Mater. Interfaces 6 (2014) 7665–7671.
[39] J. Benziger, J. Nehlsen, D. Blackwell, T. Brennan, J. Itescu, J. Membr. Sci. 261 (2005) 98–106.
[40] W.-M. Yan, D.-K. Wu, X.-D. Wang, A.-L. Ong, D.-J. Lee, A. Su, J. Power Sources 195 (2010) 5731–5734.
[41] G. Velayutham, Int. J. Hydrog. Energy 36 (2011) 14845–14850.
[42] Y. Hiramitsu, K. Kobayashi, M. Hori, J. Power Sources 195 (2010) 7559–7567.
[43] E. Antolini, R.R. Passos, E.A. Ticianelli, J. Power Sources 109 (2002) 477–482.
[44] D. Spernjak, J. Fairweather, R. Mukundan, T. Rockward, R.L. Borup, J. Power Sources 214 (2012) 386–398.
[45] P. Gallo Stampino, L. Omati, C. Cristiani, G. Dotelli, Fuel Cells 10 (2010) 270–277.
[46] R. Schweiss, M. Steeb, P.M. Wilde, T. Schubert, J. Power Sources 220 (2012) 79–83.
[47] D. Bevers, R. Rogers, M. von Bradke, J. Power Sources 63 (1996) 193–201.
[48] G. Velayutham, J. Kaushik, N. Rajalakshmi, K.S. Dhathathreyan, Fuel Cells 7 (2007) 314–319.
[49] M. Gola, M. Sansotera, W. Navarrini, C.L. Bianchi, P. Gallo Stampino, S. Latorrata, G. Dotelli, J. Power Sources 258 (2014) 351–355.
[50] S.B. Park, S. Kim, Y.I. Park, M.H. Oh, J. Phys. Conf. Ser. 165 (2009) 012046.
[51] S.-Y. Fang, L.G. Teoh, R.-H. Huang, K.-L. Hsueh, K.-H. Yang, W.-K. Chao, F.-S. Shieu, Int. J. Hydrog. Energy 39 (2014) 21177–21184.
[52] W. Song, H. Yu, Z.G. Shao, B.-L. Yi, J. Lin, N. Liu, Chin. J. Catal. 35 (2014) 468–473.
[53] E. Nishiyama, T. Murahashi, J. Power Sources 196 (2011) 1847–1854.
[54] J. Pauchet, M. Prat, P. Schott, S. Pulloor Kuttanikkad, Int. J. Hydrog. Energy 37 (2012) 1628–1641.
[55] L.M. Pant, S.K. Mitra, M. Secanelli, J. Power Sources 206 (2012) 153–160.
[56] C. Qin, D. Rensink, S. Fell, S.M. Hassanizadeh, J. Power Sources 197 (2012) 136–144.
[57] S. Pulloor Kuttanikkad, M. Prat, J. Pauchet, J. Power Sources 196 (2011) 1145–1155.

[58] B. Straubhaar, J. Pauchet, M. Prat, Int. J. Hydrogen Energy 40 (2015) 11668–11675.
[59] X.L. Liu, F.Y. Peng, G.F. Lou, Z. Wen, J. Power Sources 299 (2015) 85–96.
[60] I. Manke, C. Hartnig, M. Grünerbel, W. Lehnert, N. Kardjilov, A. Haibel, A. Hilger, J. Banhart, H. Riesermeier, Appl. Phys. Lett. 90 (2007) 174015.
[61] T.H. Haines, FEBS Lett. 346 (1994) 115–122.
[62] F. Moebius, D. Or, J. Colloid Interfaces Sci. 377 (2012) 406–415.
[63] J. Cho, J. Park, H. Oh, K. Min, E. Lee, J.-Y. Jyoung, Appl. Energy 111 (2013) 300–309.
[64] O.S. Burheim, H. Su, S. Pasupathi, J.G. Pharoah, B.G. Pollet, Int. J. Hydrog. Energy 38 (2013) 8437–8447.
[65] A. Thomas, G. Maranzana, S. Didierjean, J. Dillet, O. Lottin, Int. J. Hydrog. Energy 39 (2014) 2649–2658.
[66] W. Schmittinger, A. Vahidi, J. Power Sources 180 (2008) 1–14.
[67] D.L. Wood, S. Pacheco, J. Davey, R.L. Borup, Fuel Cell Seminar, Los Alamos National Laboratory, 2005.
[68] S. Chevalier, B. Auvity, J.C. Olivier, C. Josset, D. Trichet, M. Machmoum, Fuel Cells 14 (2014) 416–429.
[69] S.-C. Yu, X.-J. Li, J. Li, S. Liu, J.-K. Hao, Z.-G. Shao, B.-L. Yi, RSC. Adv. 4 (2014) 3852–3856.
[70] V. Parry, G. Berthomé, J.-C. Joud, Appl. Surf. Sci. 258 (2012) 5619–5627.
[71] V. Gurau, M.J. Bluemle, E.S. De Castro, Y.-M. Tsou, J. Adin Mann, T.A. Zawodzinski Jr., J. Power Sources 160 (2006) 1156–1162.
[72] J.G. Pharoah, J. Power Sources 144 (2005) 77–82.
[73] P. Mangal, L.M. Pant, N. Carrigy, M. Dumontier, V. Zingan, S. Mitra, M. Secanell, Electrochim. Acta 167 (2015) 160–171.
[74] M. Sansotera, W. Navarrini, M. Gola, G. Dotelli, P. Gallo Stampino, C.L. Bianchi, Int. J. Hydrog. Energy 37 (2012) 6277–6284.
[75] S.-C. Yu, X.-J. Li, J. Li, S. Liu, W.-T. Lu, Z.-G. Shao, B.L. Yi, Energy Convers. Manage 76 (2013) 301–306.
[76] R. Alink, D. Gerteisen, W. Mérida, Fuel Cells (11) (2011) 481–488.
[77] F. Mack, M. Klages, J. Scholta, L. Jörissen, T. Morawietz, R. Hiesgen, D. Kramer, R. Zeis, J. Power Sources 255 (2014) 431–438.
[78] M. Hara, J. Inukai, B. Bae, T. Hoshi, K. Miyatake, M. Uchida, H. Uchida, M. Watanabe, Electrochim. Acta 82 (2012) 277–283.
[79] A. Bazylak, Int. J. Hydrog. Energy 34 (2009) 3845–3857.
[80] J. Lee, J. Hinebaugh, A. Bazylak, J. Power Sources 227 (2013) 123–130.
[81] J. Eller, T. Rosén, F. Marone, M. Stampanoni, A. Wokaun, F.N. Büchi, J. Electrochem. Soc. 158 (2011) B963–B970.
[82] A. Lamibrac, J. Roth, M. Toulec, F. Marone, M. Stampanoni, F.N. Büchi, J. Electrochem. Soc. 163 (3) (2016) F202–F209.
[83] S. Hirakata, M. Hara, K. Kakinuma, M. Uchida, D.A. Tryk, H. Uchida, M. Watanabe, Electrochim. Acta 120 (2014) 240–247.
[84] I. Nitta, T. Hottinen, O. Himanen, M. Mikkola, J. Power Sources 171 (2007) 26–36.
[85] G. Dotelli, L. Omati, P. Gallo Stampino, P. Grassini, D. Brivio, J. Power Sources 196 (2011) 8955–8966.
[86] E. Sadeghi, N. Djilali, M. Bahrami, J. Power Sources 195 (2010) 8104–8109.
[87] Y.-H. Lai, P.A. Rapaport, C. Ji, V. Kumar, J. Power Sources 184 (1) (2008) 120–128.
[88] S.G. Kandlikar, Z. Lu, T.Y. Lin, D. Cooke, M. Daino, J. Power Sources 194 (1) (2009) 328–337.
[89] A. Bazylak, D. Sinton, Z.-S. Liu, N. Djilali, J. Power Sources 163 (2007) 784–792.
[90] V. Radhakrishnan, P. Haridoss, Int. J. Hydrog. Energy 35 (2010) 11107–11118.
[91] S.R. Dhanuskodi, F. Capitanio, T. Biggs, W. Merida, Int. J. Hydrog. Energy 40 (2015) 16846–16859.
[92] K.D. Baik, S.I. Kim, B.K. Hong, K. Han, M.S. Kim, Int. J. Hydrog. Energy 36 (2011) 9916–9925.
[93] K. Poornesh, C.D. Cho, G.B. Lee, Y.S. Tak, J. Power Sources 195 (2010) 2718–2730.
[94] Q.-G. Yan, H. Toghiani, Y.-W. Lee, K.-W. Liang, H. Causey, J. Power Sources 160 (2006) 1242–1250.
[95] C. Lee, W. Mérida, J. Power Sources 164 (2007) 141–153.
[96] S.-Y. Lee, H.-J. Kim, E. Cho, K.-S. Lee, T.-H. Lim, C. Hwang, H.J. Jong, Int. J. Hydrog. Energy 35 (2010) 12888–12896.
[97] R. Mukundan, Y.-S. Kim, T. Rockward, J.R. Davey, B.S. Pivovar, D.S. Hussey, D.L. Jacobson, M. Arif, R.L. Borup, ECS Trans. 11 (2007) 543–552.
[98] S. Kim, C. Chacko, R.P. Ramasamy, M.M. Mench, ECS Trans. 11 (2007) 577–586.
[99] Y. Lee, B. Kim, Y. Kim, X.-G. Li, J. Power Sources 196 (2011) 1940–1947.
[100] J.H. Chun, D.H. Jo, S.G. Kim, S.H. Park, C.H. Lee, S.H. Kim, Renew. Energy 48 (2012) 35–41.
[101] S. Latorrata, P. Gallo Stampino, C. Cristiani, G. Dotelli, Int. J. Hydrog. Energy 40 (2015) 14596–14608.
[102] J.-F. Wu, J.J. Martin, F.P. Orfino, H.-J. Wang, C. Legzdins, X.-Z. Yuan, C. Sun, J. Power Sources 195 (2010) 1888–1894.
[103] S.G. Kandlikar, M.L. Garofalo, Z. Lu, Fuel Cells 11 (2011) 814–823.
[104] Z.J. Lu, M.M. Daino, C. Rath, S.G. Kandlikar, Int. J. Hydrog. Energy 35 (2010) 4222–4233.
[105] J. Fairweather, B. Li, R. Mukundan, J. Fenton, R. Borup, ECS Trans. 33 (2010) 433–446.
[106] J. Cho, T. Ha, J. Park, H.-S. Kim, K. Min, E. Lee, J.-Y. Jyoung, Int. J. Hydrog. Energy 36 (2011) 6090–6098.
[107] J. Frisk, W. Boand, M. Kurkowski, R. Atanasoski, A. Schmoeckel, Fuel Cell Seminar, 2004. San Antonio (TX).
[108] T. Aoki, A. Matsunaga, Y. Ogami, A. Maekawa, S. Mitsushima, K.-I. Ota, H. Nishikawa, J. Power Sources 195 (2010) 2182–2188.
[109] J. Healy, C. Hayden, T. Xie, K. Olson, R. Waldo, M. Brundage, H. Gasteiger, J. Abbott, Fuel cells 5 (2005) 302–308.
[110] C.A. Reiser, L. Bregoli, T.W. Patterson, J.S. Yi, J.D.L. Yang, M.L. Perry, T.D. Jarvi, Electrochem. Solid State Lett. 8 (2005) A273–A276.
[111] A. Lamibrac, G. Maranzana, O. Lottin, J. Dillet, J. Mainka, S. Didierjean, A. Thomas, C. Moyne, J. Power Sources 196 (2011) 9451–9458.
[112] G.B. Chen, H.M. Zhang, H.P. Ma, H.X. Zhong, Int. J. Hydrog. Energy 34 (2009) 8185–8192.
[113] R. Mukundan, J.R. Davey, K. Rau, D.A. Langlois, D. Spernjak, J.D. Fairweather, K. Artyushkova, R. Schweiss, R.L. Borup, ECS Trans. 58 (2013) 916–926.
[114] R. Lin, F. Xiong, W.C. Tang, L. Techer, J.M. Zhang, J.X. Ma, J. Power Sources 260 (2014) 150–158.
[115] J. Shan, R. Lin, S. Xia, D. Liu, Int. J. Hydrog. Energy 41 (2016) 4239–4245.
[116] B.-T. Huang, Y. Chatillon, C. Bonnet, F. Lapicque, S. Leclerc, M. Hinaje, S. Raël, Fuel Cells 12 (2012) 335–346.
[117] J. Hao, S. Yu, Y. Jiang, X. Li, Z. Shao, B. Yi, J. Electroanal. Chem. 756 (2015) 201–206.
[118] J. Lobato, H. Zamora, P. Canizares, J. Plaza, M.A. Rodrigo, J. Power Sources 288 (2015) 288–295.
[119] A. Bottino, G. Capanelli, A. Comite, C. Costa, A.L. Ong, Int. J. Hydrog. Energy 40 (2015) 14690–14698.
[120] F.-B. Weng, C.-Y. Hsu, M.-C. Su, Int. J. Hydrog. Energy 36 (2011) 13708–13714.
[121] J.M. Morgan, R. Datta, J. Power Sources 251 (2014) 269–278.
[122] T. Kitahara, H. Nakajima, M. Inamoto, K. Shinto, J. Power Sources 248 (2014) 1256–1263.
[123] A. Forner-Cuenca, J. Biesdorf, L. Gubler, P.M. Kristiansen, T.J. Schmidt, P. Boillat, Adv. Mater. 27 (2015) 6317–6322.
[124] T. Kitahara, H. Nakajima, M. Inamoto, M. Morishita, J. Power Sources 234 (2013) 129–138.